Chapter 8

NHANSIPFE GRANITIC ORTHOGNEISS

8.1 Introduction

The Nhansipfe Granitic Orthogneiss is exposed east of the Vanduzi Migmatite Gneiss and west of the Chimoio Granodioritic Gneiss (Fig. 2.1). Previous work did not differentiate this granite from the Messica Granite Gneiss. During the present study mineralogical and textural characteristics, on outcrop scale, enabled its distinction from the Messica Granite Gneiss. A Rb/Sr isotope study confirms the distinction and indicates that the Nhansipfe Granitic Orthogneiss is much younger.

8.2 Field Description

A common characteristic of the granitoids of this unit is the megacrystic size of feldspar crystals. The rock type is commonly an augen gneiss, locally with intercalations of quartzo-feldspathic partial melt bands and pegmatitic veins (Figs. 8.1 and 8.2). The mineralogy includes feldspar, quartz and garnet and biotite and hornblende in the felsic and mafic bands respectively. Garnet occurs as medium-grained aggregates and coarse isolated grains that are locally idioblastic, particularly within the felsic bands. Some feldspar grains, commonly the largest ones, are also idioblastic. The foliation is defined by the preferred orientation of biotite and is deformed around the coarse feldspars porphyroclasts and commonly includes NE-SW S_1 and an approximately N-S S_2 foliations (Fig. 8.3). At Matsinho, the gneiss is intensely folded(Fig. 8.4) and contains mafic fine-grained gneissic enclaves composed of plagioclase, pyroxene, hornblende, and garnet which suggests that the grantoids intruded a mafic rock.

Figure 8.1: Quartzo-feldspathic partial melt bands in the megacrystic Nhansipfe Granitic Orthogneiss.

Figure 8.2: Pegmatitic veins forming intercalated bands in the megacrystic Nhansipfe Granitic Orthogneiss.

Figure 8.3: S_1 and S_2 foliations in the megacrystic Nhansipfe Granitic Orthogneiss near Mombeza.

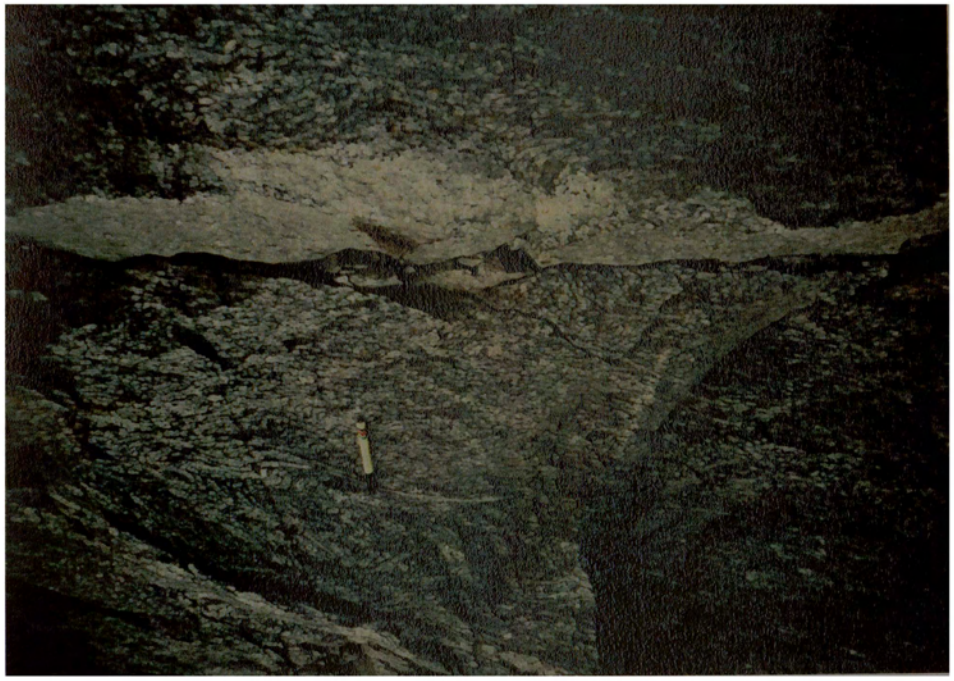

Figure 8.4: Folded foliation in the fine-grained light-coloured gneiss in Matsinho.

Figure 8.5: Folded felsic bands offset by subvertical faults in the megacrystic Nhansipfe Granitic Orthogneiss.

The megacrystic rock is folded, the folds being defined by the felsic bands which are locally offset by subvertical faults (Fig. 8.5). At Chibata, the gneiss contains mafic enclaves consisting of plagioclase, hornblende, pyroxene and garnet. These enclaves are massive fine-grained at the core but, at the contact with the gneiss, are foliated. The gneiss is sheared as indicated by feldspar stretching (Fig. 8.6) and mesoboudins in mafic enclave (Fig. 8.7). Feldspar porphyroclasts suggest a sinistral movement.

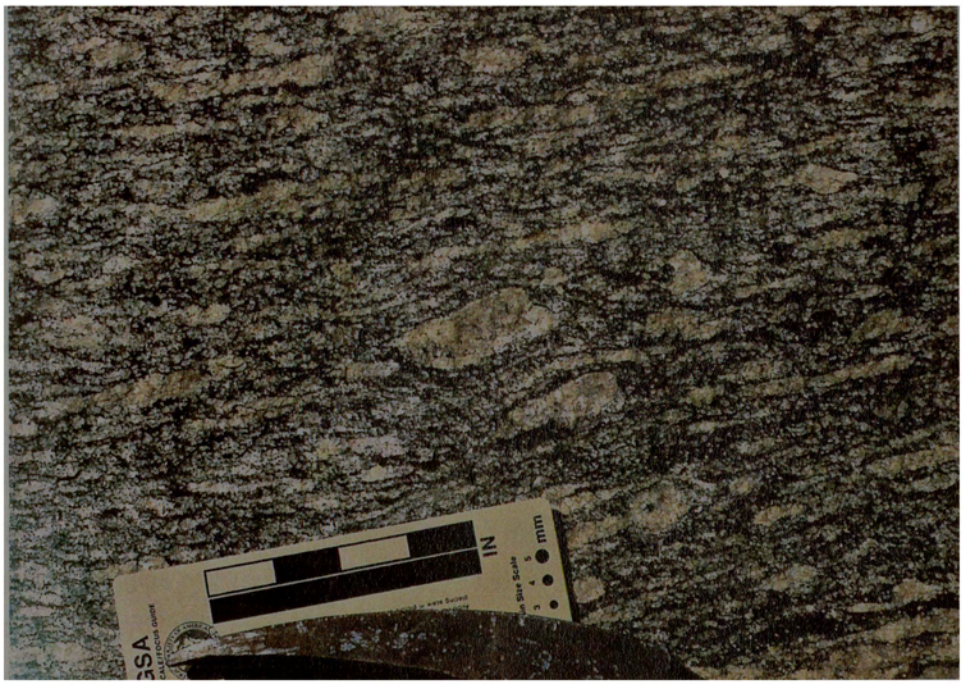

Figure 8.6: Sinistral feldspar porphyroclasts in the megacrystic gneiss near Chibata.

Figure 8.7: Mesoboudins in the mafic enclaves in the megacrystic gneiss near Chibata.

8.3 Petrography

The estimated modes of the minerals in this gneiss are shown in Table 8.1. The mineralogy is dominated by alkali and plagioclase feldspar and quartz. Biotite and hornblende occur in lesser amounts and garnet, titanite, zircon and opaque minerals are accessories. In the Nhansipfe (samples nfgn's) and Mombeza (samples mrgn and mggn's) localities, hornblende is absent. The opaque minerals occur in all samples but their proportions are higher in those samples enriched in ferromagnesian minerals. The rocks are generally inequigranular and are characterised by very coarse-grained feldspar(>3 cm). Samples from the Matsinho (samples mhgn's) and Chibata (samples pcy and grf) localities are fine- to medium-grained possibly due to grain-size reduction caused by deformation. The rocks are generally characterized by a planar fabric defined by the preferred orientation of biotite and/or hornblende. Alternating bands of felsic and mafic minerals, define compositional layering. The texture in the felsic bands is essentially coarse-grained granoblastic whereas within the mafic bands the texture is medium-grained lepidoblastic.

K-feldspar and plagioclase occur as coarse xenoblastic grains. Plagioclase grains are commonly zoned and contain inclusions of finer feldspar and quartz grains. Some are cracked and commonly contain fine grains of sericite and epidote. The coarse feldspars are deformed and elongated along foliation planes and locally form mosaics of non-zoned grains with granoblastic grain boundaries with interfacial angles of about 120°. Locally, the K-feldspar exhibits perthitic textures whereas plagioclase shows antiperthitic intergrowths. Quartz is anhedral and commonly contains inclusions of feldspar. Coarse grains of quartz have undulose extinction and are often partially recrystallised around their margins to fine-grained granoblastic mosaics thereby defining a mortar texture. Quartz is locally intergrown with plagioclase forming myrmekite which partially replaces microcline (Fig. 8.8). Hornblende forms anhedral grains and are generally cracked. The grains contain inclusions of quartz, zircon, titanite and opaque minerals. Some grains show preferred orientation and are deformed and oriented along foliation planes. Biotite occurs as aggregates or isolated flakes and is generally spatially associated with hornblende. In some samples, biotite is the only ferromagnesian phase but when hornblende is present they seem to occur in similar proportions. Biotite flakes exhibit preferred orientation along foliation planes (Fig. 8.9). Garnet is spatially associated with both felsic and ferromagnesian. It occurs as fine grains which are commonly idioblastic, particularly when filling cracks in both feldspar and hornblende. It is also present as coarse xenoblastic grains along grain boundaries or as inclusions in plagioclase and ferromagnesian minerals. Coarse garnet grains are commonly cracked and locally appear mantled by hornblende (Fig.8.10).

Table 8.1: Modal proportion of minerals in the Nhansipfe Granitic Orthogneiss.

sample	K-fld	Plg	Qtz	Hbl	Bt	Ms	Grt	Ttn	Zrn	Ap	Opm
nfgn1	27	34	28	-	10	-	-	-	tr	-	1
nfgn2	30	32	27	-	7	-	2	-	1	-	1
nfgn3	28	30	28	-	10	-	2		1	-	1
nfgn4	28	32	26	-	10	-	2	-	1	-	1
nfgn5	30	33	25	-	8	-	2	-	1	-	1
nfgn6	30	30	26	-	8	-	2	-	1	-	1
mggn1	27	30	28	-	8	-	4	-	1	-	2
mggn2	26	29	30	-	10	-	4		-	-	1
nggn2	30	28	30	-	8	1	2		-	-	1
ndgn1	30	28	30		8	1	3	-	-	-	-
nzgg1	30	30	28	4	6	-		-	1	-	1
nzgn2	28	32	28	4	5	-	-	1	1	-	1
nzgn3	30	30	28	5	5	-	-	-	1	-	1
mrgn	30	33	26	-	8	-	3	-	-	-	-
chgn	30	32	28	-	8	-	2	-	-	-	-
mhgn1	25	28	25	12	8	-	-	-	1	tr	1
mhgn2	23	30	25	10	10	-	-	tr	1	tr	1
mhgr	26	24	30	12	7	-	-	-	-	-	1
mhgn6	25	23	27	12	10	-	-	tr	1	-	2
agn1	30	35	25	4	5	-	-	-	-	tr	1
agn2	30	33	25	5	4	-	-	2	-	tr	1
agn3	28	32	24	8	6	-	-	1	-	-	1
agn4	30	34	25	5	2	-	-	2	-	-	2
agn5	25	30	28	8	2	-	-	2	tr	tr	3
agn6	28	30	28	6	3	-	-	2	-	-	3
pcy	30	30	32	3	1	-	-	tr	1	-	3
mcgr	27	30	28	12	8	-	-	-	tr	-	3

Plg-plagioclase, K-fld- potassium-feldspar, Qtz- quartz, Hbl- hornblende, Bt- biotite, Ms- muscovite, Grt-garnet, Ttn- titanite, Zrn- zircon, ap- apatite and Opm- opaque minerals; tr=trace.

Figure 8.8: Myrmekitic intergrowths in the Nhansipfe Granitic Orthogneiss. Minerals in the photo are microcline (cross-hatch twinning), plagioclase (dark grey) and quartz (yellowish white). Crossed nicols, width of field 3 mm.

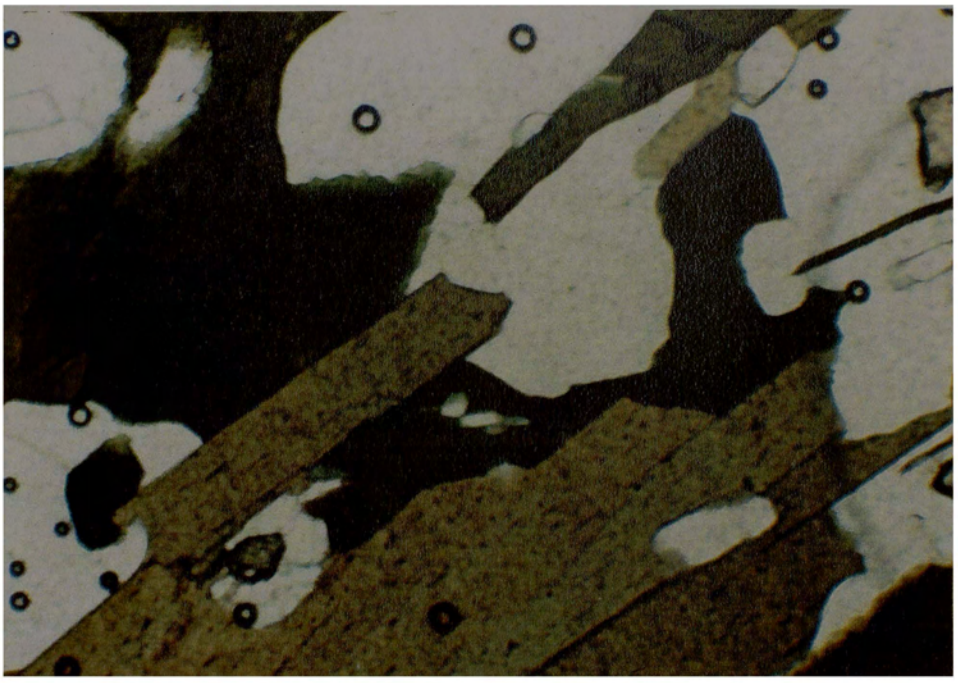

Figure 8.9: Biotite flakes forming planar foliation. Parallel light, width of field 3 mm. Circular spots are air bubles in the epoxy resin.

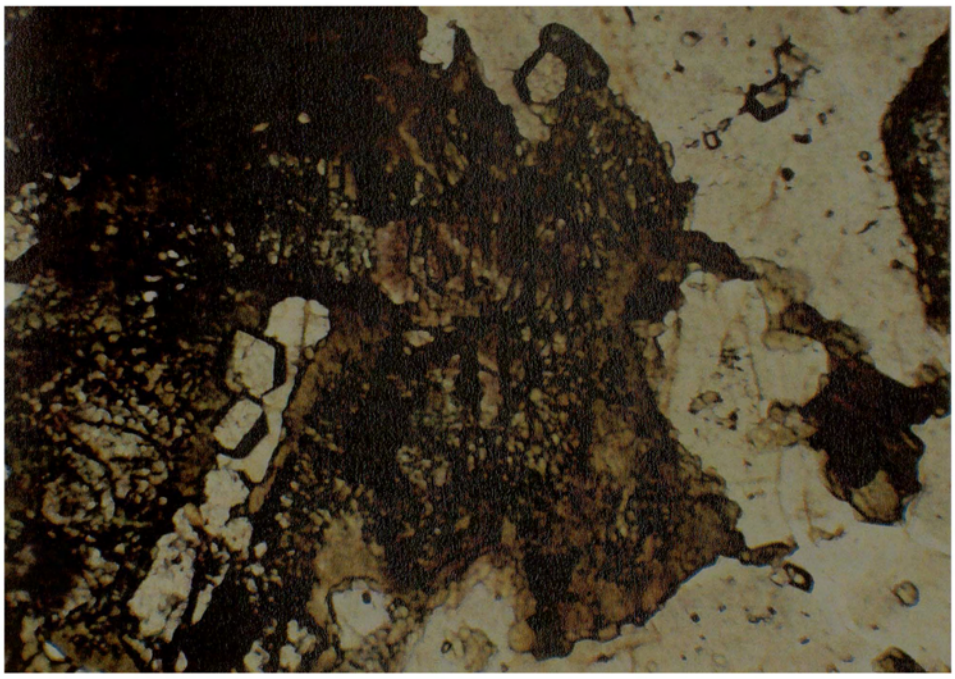

Figure 8.10: Hornblende (brown) mantled xenoblastic and cracked garnet and idioblastic garnet grains (high relief) along plagioclase cracks from the Nhansipfe granitoids. Parallel light, width of field 7 mm.

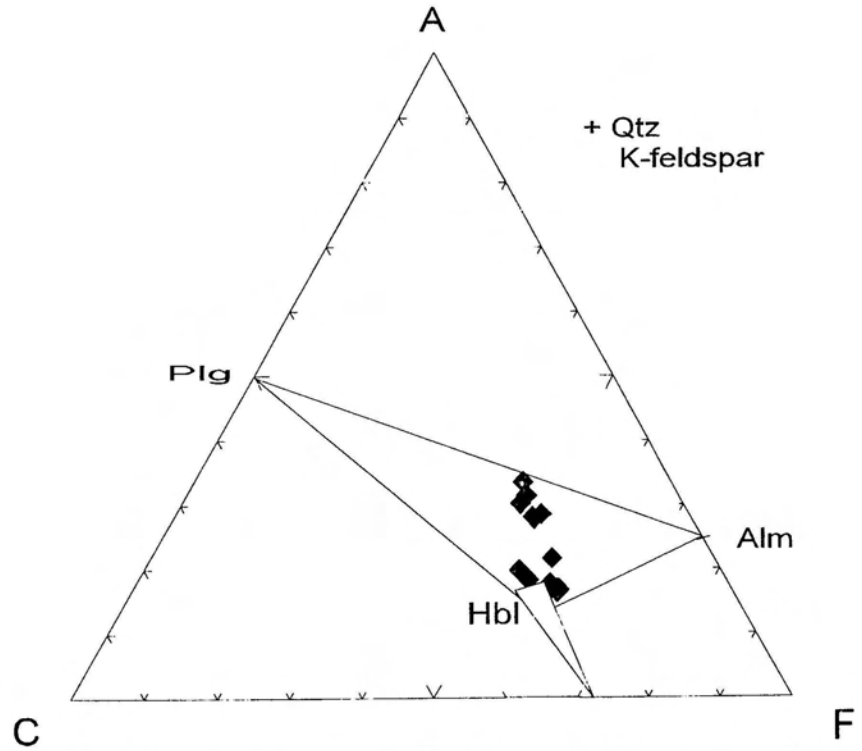

Figure 8.11: ACF diagram plotting the chemistry and showing the equilibrium mineral assemblage of medium-grade amphibolite facies of Nhansipfe Granitic Orthogneiss. Hbl- hornblende, Alm- almandine, Qtz- quartz, K-feldspar- potassium feldspar and Plg- plagioclase.

Titanite is a common accessory mineral in samples enriched with ferromagnesian minerals and is spatially associated with them as fine to coarse-grains. It is also associated with plagioclase. Coarse grains of titanite generally contain inclusions of felsic minerals. Zircon occurs as isolated prismatic grains as inclusions in both felsic and mafic minerals. Apatite is rare but occurs as hexagonal grains usually included in felsic minerals. Opaque minerals occur as sub- to anhedral grains in two ways, namely, as isolated and interstitial grains or grains associated with ferromagnesian minerals.

8.3.1 Interpretation of Petrography

Besides quartz and K-feldspar, the Nhansipfe Granitic Orthogneiss is characterised by the mineral assemblage of plagioclase±hornblende±garnet±biotite (Fig. 8.11). The co-existence of hornblende+garnet+plagioclase (composition ~An_{20}) is typical of medium grade or amphibolite facies metamorphism. The preservation of complex Carlsbad/albite polysynthectic twinning in plagioclase would support an igneous origin for the gneiss (Smith and Mackenzie, 1959). The perthitic textures in orthoclase and antiperthitic textures in plagioclase suggest that the rocks had been subjected to higher temperatures, and have cooled down sufficiently slowly to permit the development of these exsolution textures.

In Figure 8.10, xenoblastic garnet is mantled by hornblende which is in contact with plagioclase, suggesting that the hornblende is produced by a hydration reaction involving garnet and plagioclase. On the other hand, the idioblastic garnet grains could have been produced by a prograde metamorphic reaction involving plagioclase and hornblende. The fact that this garnet does not show any reaction texture, suggests that it was produced at a later stage than the xenoblastic garnet and consequently this would suggest three metamorphic episodes, namely (1) prograde metamorphism to medium-grade amphibolite facies producing garnet and hornblende, (2) retrograde (hydration) metamorphism (reaction of garnet to produce hornblende) and (3) prograde metamorphism (reaction of plagioclase and hornblende to produce the idiomorphic garnet grains).

8.4 Chemistry

8.4.1 Introduction

The major and trace element compositions of 15 analysed samples are shown in Table 8.2 . The rare earth element (REE) compositions of four samples and the Rb/Sr isotopic data are shown in Table 8.3 and 8.4 respectively.

Table 8.2: Major and trace element analyses of samples from the Nhansipfe Granitic Orthogneiss.

SAMPLE	NFGN1	NFGN2	NFGN3	NFGN4	NFGN5	NFGN6	AGN1	AGN3	NZGN	MHGN1	MHGN2	MHGN3	MHGN4	MHGN5	MHGN6
SiO_2	66.11	66.16	66.2	65.95	65.47	65.45	66.3	66.74	65.31	63.3	63.35	63.31	62.67	67.49	63.39
Al_2O_3	15.56	15.36	15.62	15.07	15.63	15.65	14.43	14.57	13.71	14.21	14.08	14.18	14.44	13.62	14.39
Fe_2O_3	2.03	2.28	1.92	2.26	2.17	2.13	2.48	2.34	2.80	3.46	3.54	3.40	3.38	2.67	3.39
FeO	2.88	3.26	2.93	3.38	2.91	3.12	3.00	2.90	4.14	4.82	4.69	4.69	4.70	3.31	4.57
MgO	1.18	1.37	1.28	1.46	1.34	1.32	1.08	1.11	1.26	1.49	1.58	1.47	1.47	0.98	1.54
CaO	2.69	2.83	2.78	3.11	2.87	3.13	3.19	3.27	3.2	3.86	4.15	3.75	3.9	2.88	3.81
Na_2O	2.78	2.98	2.76	3.00	2.98	2.94	3.40	3.44	2.85	3.45	3.77	3.54	3.49	3.26	3.66
K_2O	4.18	3.92	3.54	3.52	4.51	3.74	4.97	4.72	3.76	3.85	3.95	3.84	3.83	4.81	3.91
TiO_2	0.64	0.76	0.74	0.84	0.78	0.73	0.97	0.91	1.06	1.25	1.33	1.25	1.2	0.85	1.3
P_2O_5	0.21	0.27	0.24	0.27	0.26	0.25	0.25	0.24	0.28	0.33	0.34	0.33	0.3	0.21	0.34
MnO	0.06	0.06	0.04	0.05	0.04	0.06	0.1	0.1	0.11	0.14	0.16	0.15	0.14	0.11	0.16
total	98.32	99.25	98.05	98.91	98.96	98.52	100.17	100.34	98.48	100.16	100.94	99.91	99.52	100.19	100.46
Ba	1008	978	747	710	1080	1101	1991	1920	1523	1969	2317	2373	2033	2101	2404
Li	33	41	33	36	36	33	23	24	28	29	23	19	24	28	19
Nb	32	34	34	40	37	34	33	31	32	41	34	32	39	27	33
Sc	8	9	7	8	7	9	14	14	15	18	19	16	16	13	17
Sr	259	250	217	222	259	307	364	365	281	325	391	391	345	299	407
Rb	212	216	211	199	219	209	137	127	99	88	86	106	100	101	82
Y	38	27	22	37	24	27	87	81	81	81	74	69	85	72	72
Ga	23	21	24	24	22	24	21	20	22	22	21	22	23	20	23
Al	8	8	8	8	8	8	8	8	7	8	8	8	8	7	8
Zr	278	295	420	346	319	327	498	395	524	792	743	793	719	620	737

8.4.2 Major Element Chemistry.

The SiO_2 contents of the samples are typically acid (granitic). The samples are enriched in Al_2O_3 with contents and FeO_{total} contents are significantly greater than the MgO contents (~1-1.5wt%) resulting in high Fe/Mg ratios of ~5:1. CaO contents are low. Total alkali contents are >6 wt% with K_2O typically being >Na_2O. Calculation of the parameter $Al_2O_3/CaO+Na_2O+K_2O$ shows that the samples from Nhansipfe locality (nfgn's) are peraluminous (A/CNK >) whereas the remaining are metaluminous (A/CNK <1). The TiO_2 contents are high and vary between 0.64-1.33 wt%. The P_2O_5 contents vary between 0.2-0.3 wt%. Harker variation diagrams of CaO and FeO_{total} contents plotted against SiO_2 show that they decrease with increasing SiO_2 contents resulting in inverse or negative correlations (Fig. 8.12). Similarly TiO_2 and P_2O_5 show decreasing contents with increasing SiO_2 whereas K_2O increases with increasing SiO_2 (Fig. 8.13).

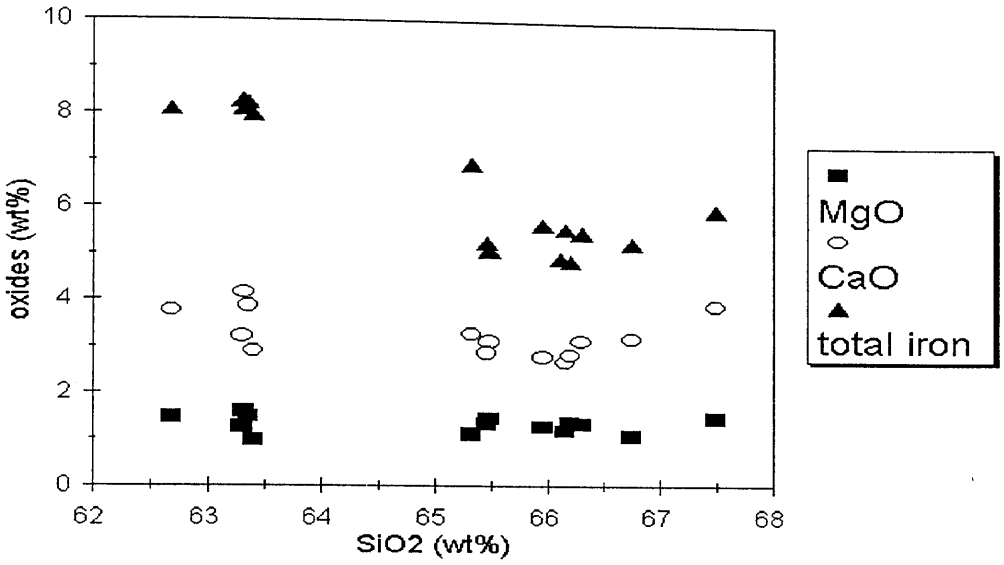

Figure 8.12: Harker variation diagram of MgO, CaO and total iron versus SiO_2 of samples from the Nhansipfe Granitic Gneiss.

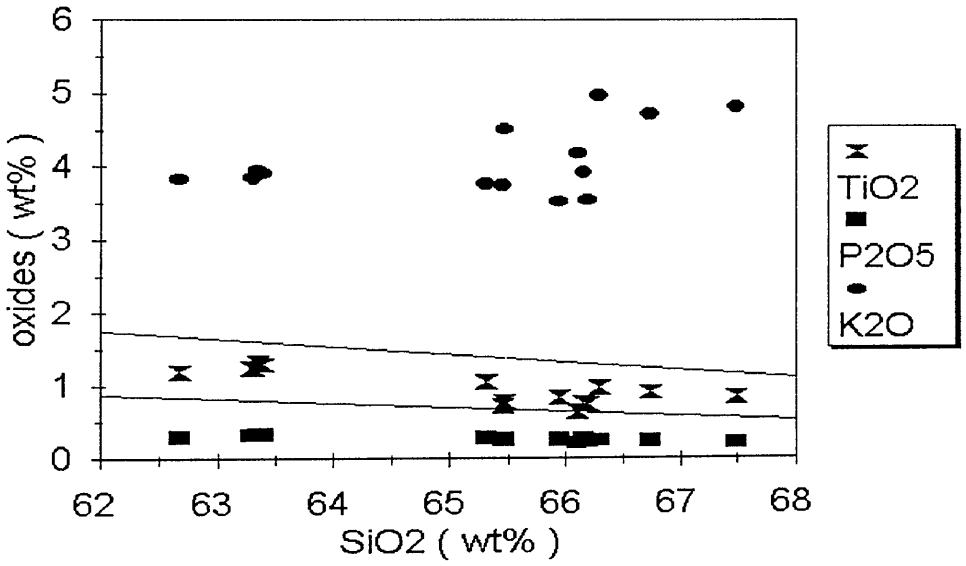

Figure 8.13: Harker variation diagram of TiO_2, P_2O_5 and K_2O vesus SiO_2 from Nhansipfe Granitic Gneiss. Shown are lines of 900 °C and 1000 °C (for 7.5 Kbar) drawn on the basis of TiO_2 contents according to Green and Pearson (1986).

Experimental work by Green and Pearson (1986) on the solubility of TiO_2 in magmas of varying compositions suggests the magma from which the Nhansife Granite originally crystallised was relatively hot, possibly of the order of 900°C. In Fig. 8.13 this is illustrated by lines of 900 °C and 1000 °C drawn on the basis of TiO_2 contents of the analysed samples, and a pressure of 7.5 kbar and according to experiments by Green and Pearson (1986). Similarly, application of saturation surface thermometry utilising the P_2O_5 contents in the samples and the calibration of the solubility of P_2O_5 in magmas of varying SiO_2 contents by Harrison and Watson (1984) suggests that the Nhansife Granite magma had a minimum temperature of ~950-1000 °C (Fig. 8.14) assuming that all the P_2O_5 is partitioned into apatite in stoichiometric proportions and that the apatite enrichment is not a result of crystal accumulation or xenocrystic incorporation. The crystal accumulation is discounted because of the similar contents in rocks of varying SiO_2 composition.

8.4.3 Trace Element Chemistry

The samples typically have high contents of Ba, Zr, Sr, Rb, Nb and Y. The high Zr contents can also be ascribed to high solubility of Zr in high temperature magmas. Zr saturation surface thermometry after Watson and Harrison (1983) indicates that the contents of Zr in the samples would require temperatures of ~800-950 °C (Fig. 8.14) assuming again that the high Zr contents are not the consequence of crystal accumulation or xenocrystic inclusion in the magma. Sr/Rb ratios are low resulting from the relatively high Rb contents, and do not show any systematic variation between ~1:1 and ~3:1. Similarly, the Y/Nb ratio is variable between ~1:1 and ~3:1. The Ba-Sr-Rb contents of the Nhansife gneisses are typical of anomalous granites (Fig. 8.15) suggesting that processes such as metasomatism might have affected the normal distribution of these elements (El Bouseilly and El Sokkary, 1975). The high Rb, Nb and Y contents are typical of within-plate granitoids (Pearce *et al*. 1984) (Fig. 8.16).

8.4.4 REE Chemistry

Four samples were analysed for the rare earth elements (REE) and their contents are shown in Table 8.3. The REE contents are high in Ce, Nd and La.

Table 8.3. Rare earth element analyses of the Nhansife Granitic Orthogneiss in ppm.

Sample	La	Ce	Pr	Nd	Sm	Eu	Gd	Dy	Ho	Er	Yb	Lu
NFGN1	75	147	16	55	8	1	6	6	1	2	2	0
NFGN2	69	136	15	53	8	1	6	5	1	2	2	0
MHGN1	65	150	20	81	15	4	14	13	2	6	6	1
MHGN2	72	154	19	78	14	4	12	11	2	5	5	1

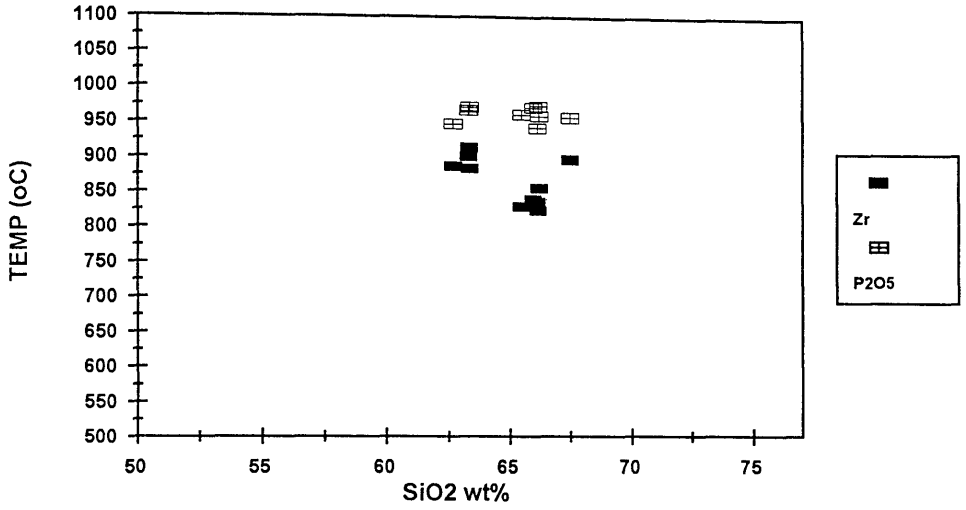

Figure 8.14: Saturation surface thermometry utilising the analysed P_2O_5 and Zr contents of the analysed samples and the solubility calibrations after Harrison and Watson (1984) and Watson and Harrison (1983).

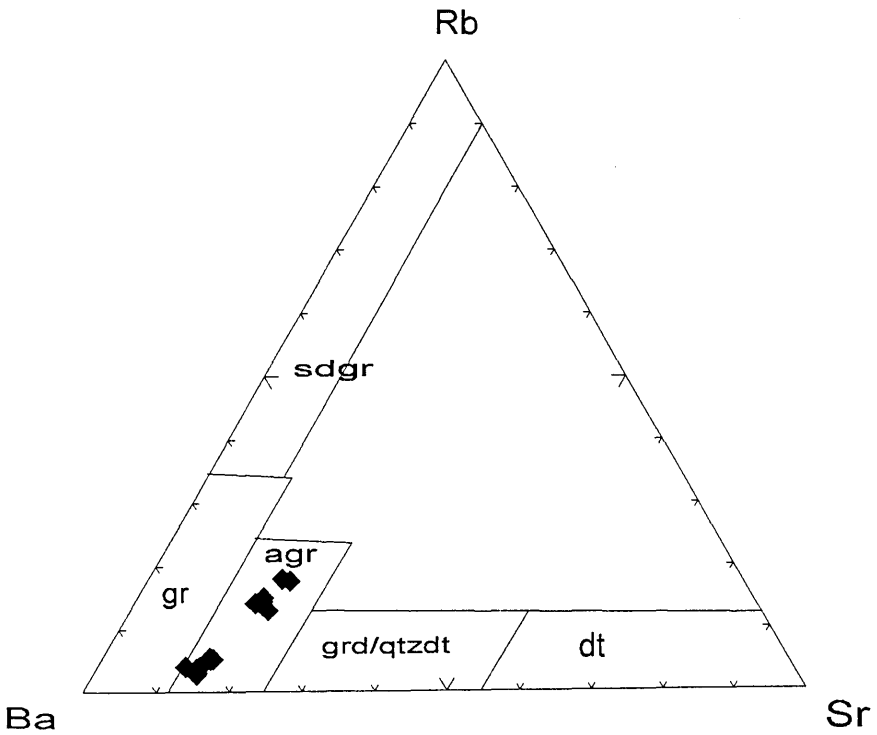

Figure 815: Chemical data plotting in the field of anomalous granites in the diagram after El Bouseily and El Sokkary (1975). Sdgr- strongly differentiated granites; gr- normal granites; agr- anomalous granites; grd- granodiorites; qtzdt- quartz diorites and dt- diorites.

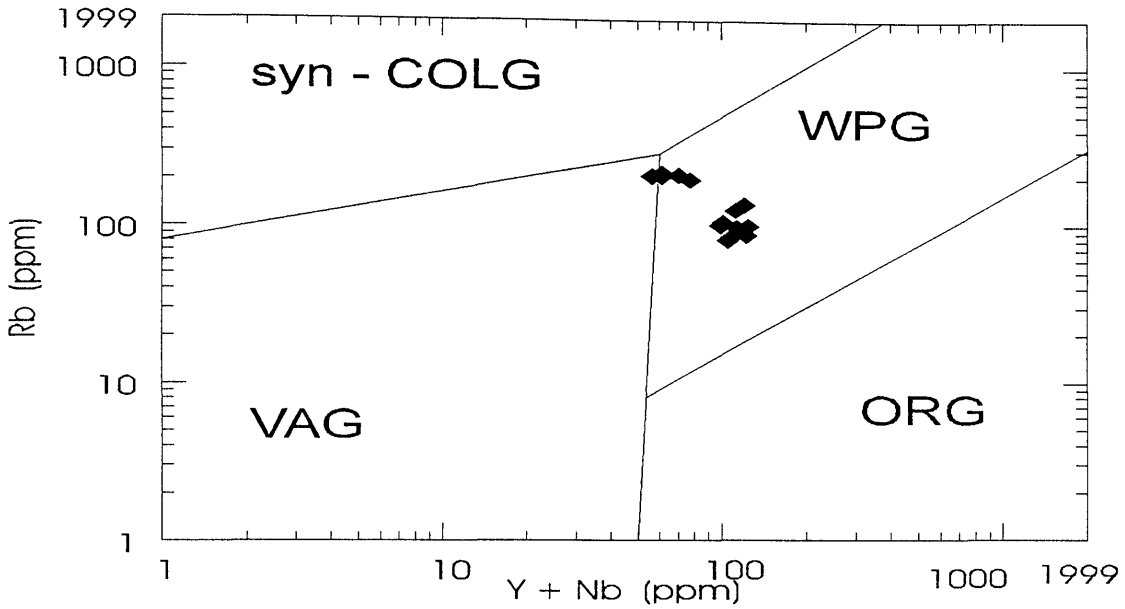

Figure 8.16:Tectonic discriminant diagram of Pearce *et al.* (1984) in which the chemical data of Nhansipfe Granitic Orthogneiss polt in the field of within-plate granitoids. Syn-COLG- syn-collision granites, VAG- volcanic-arc granites, ORG- orogenic granites, WPG- within-plate granites.

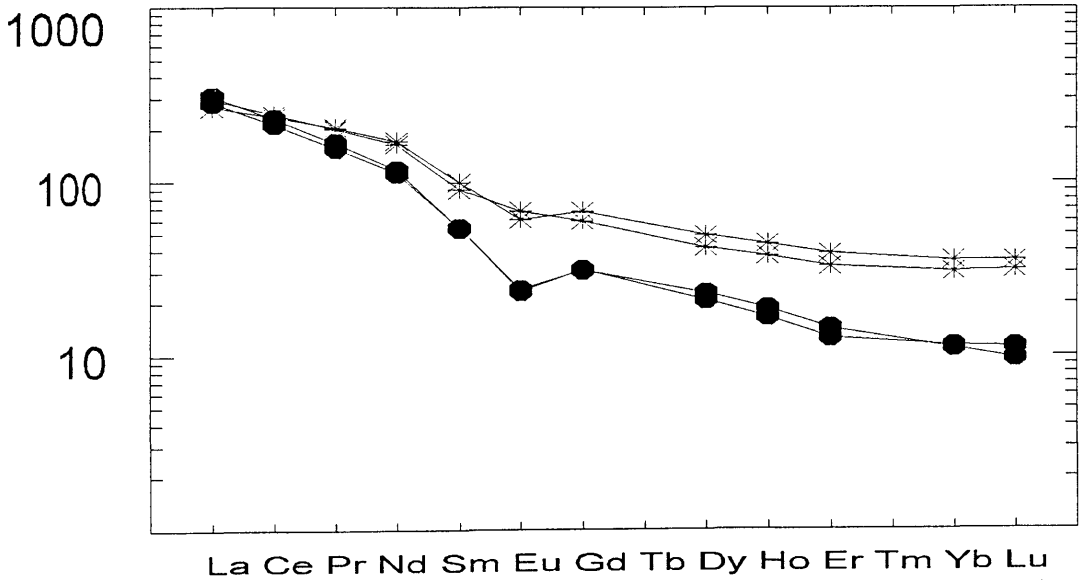

Figure 8.17: REE abundance variation diagram of the Nhansipfe Granitic Orthogneiss. Normalizing values are from Evensen *et al.* (1978) Filled boxes are samples from Nhansipfe and asterix from Matsinho localities respectively.

The conventional chondrite-normalised REE patterns for the 4 samples are shown in Figure 8.17. The REE patterns of the Nhansipfe Granitic Gneisses show a relative enrichment of the LREE relative to the HREE and are characterised by a weak to prominent negative Eu anomaly which is accentuated in the samples from the Nhansipfe locality. These negative Eu anomalies suggests either significant plagioclase feldspar in the restite or depletion of Eu from an evolving magma by fractional crystallization of plagioclase.

8.4.5 Radiogenic Rb/Sr isotope chemistry

A study of the Rb/Sr isotopes was conducted on the 6 samples labelled NFGN 1-6 (Table 8.4). Regression of the data from the 6 samples using the GEODATE (Harmer and Eglington, 1987) using 1% and 0.01% errors for the X and Y values respectively yields an errorchron of 969Ma ± 141 (MSWD 7.711) with R_o=0.7158. Exclusion of the data for sample nfgn2 from the calculation does not significantly alter the age or the R_o and results in an isochron of 981 Ma±83 Ma (MSWD=1.24) with R_o=0.7157 (Fig. 8.18). This age is clearly significantly different to that obtained for the Messica Granite Gneiss to the west.

Table 8.4. Rb/Sr trace element and isotope data from the Nhansife Granitic Gneiss.

sample	Rb(ppm)	Sr(ppm)	$^{87}Rb/^{86}Sr$	$^{87}Sr/^{86}Sr$
nfgn1	211.7	256	2.4023	0.7492
nfgn2	223.1	245.6	2.6392	0.7509
nfgn3	213	232.9	2.6576	0.7525
nfgn4	204.5	211.6	2.8092	0.7552
nfgn5	225.6	251.6	2.6057	0.7527
nfgn6	212.3	297.9	2.0694	0.7448

8.4.6 Discussion and Interpretation of Chemistry

The Nhansipfe granitoids are characterised by high abundance of alkalis, ∑FeO, Fe/Mg ratios and enrichment of Ga, Rb, Nb, Y, Zr, and REE (except Eu) and relatively lower contents of Al_2O_3, MgO, CaO and Sr. These characteristics are typical of A-type granitoids (Whalen, *et al.* 1987; Eby, 1990, 1992). These authors have further utilised various combinations of Zr, Nb, Ce, Y and Ga with CaO and Al_2O_3 to discriminate A-type granites and to subdivide these granites further. The (K_2O+Na_2O/CaO) versus (Zr+Nb+Ce+Y) diagram of Whalen *et al.* (1987) confirms the A-type nature of the granitoids in spite of the fact that Ce data are not available for all the samples (Fig. 8.19). A diagram plotting Zr versus Ga/Al is also considered a very good genetic discriminant for A-type granitoids rocks and has been used successfully by Whalen *et al.* (1987). Data form the present study plot in the field of A-type (Fig. 8. 20).

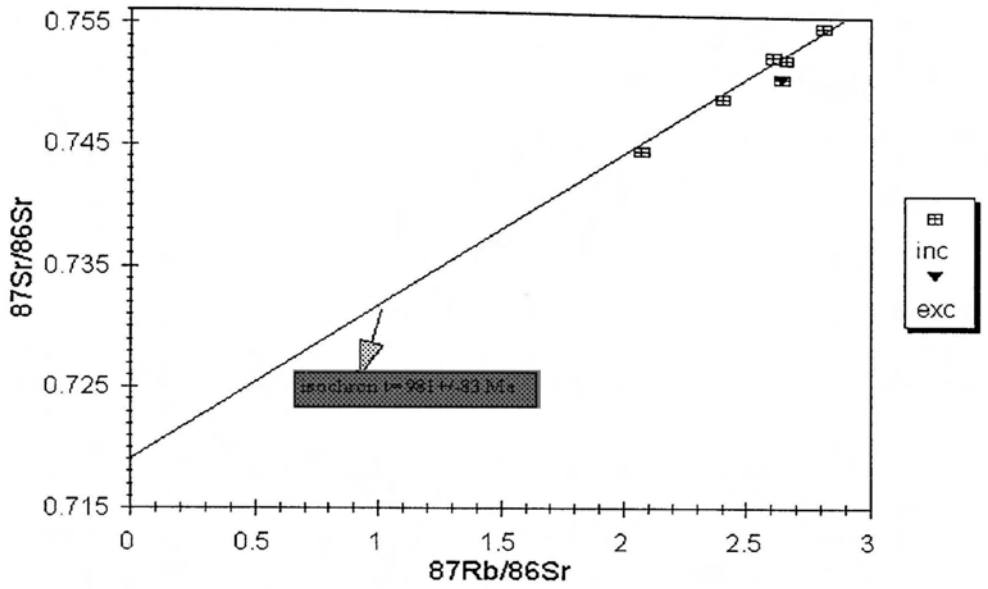

Figure 8.18: Diagram plotting radiogenic isotopic data of Nhansipfe Granitic Orthogneiss. Shown also is the isochon t=981±83 Ma. inc and exc stand for data included and excluded from the regression respectively.

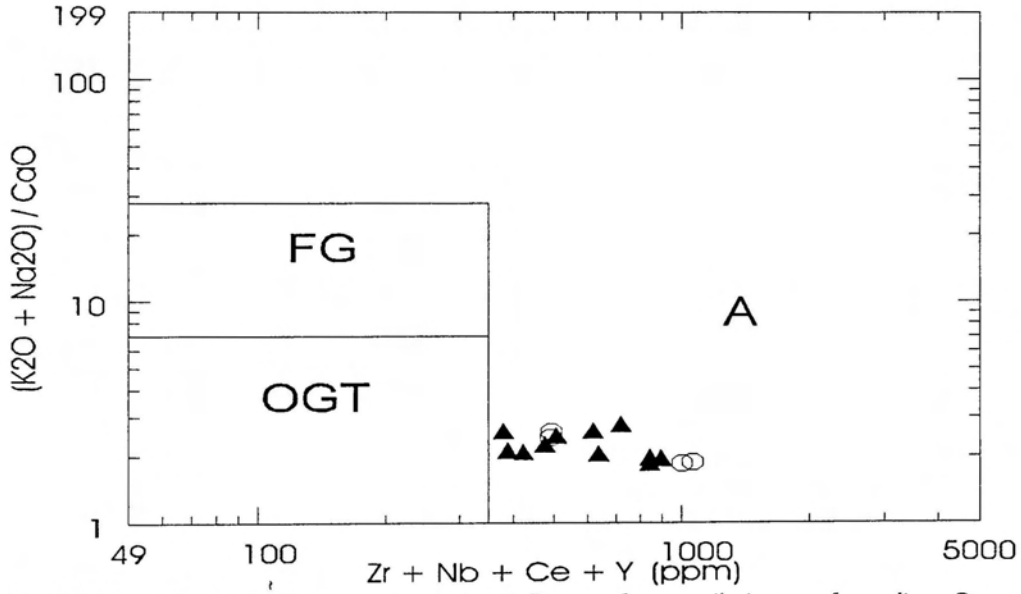

Figure 8.19: Whalen *et al.* (1987) discriminant diagram for genetic types of granites. Open circles represent samples that were analysed for REE including Ce. A- A-type granite field. FG- fractionated felsic granites and OGT- unfractionated orogenic granites.

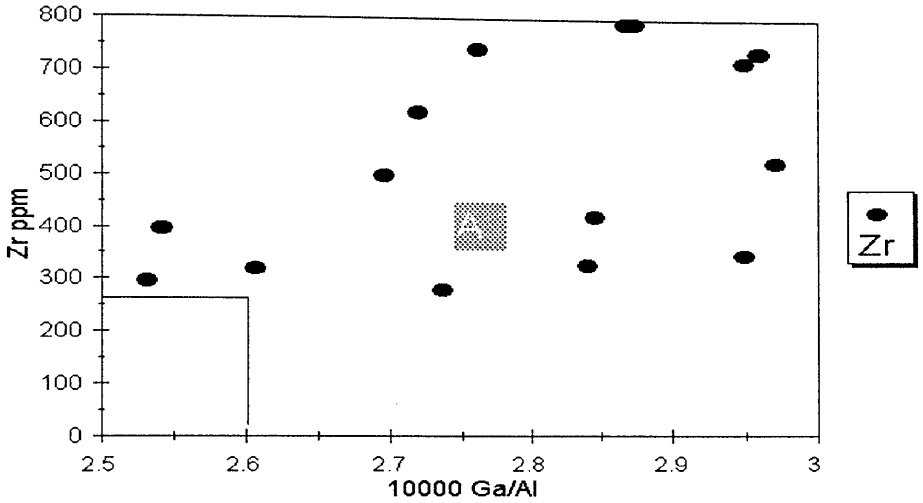

Figure 8.20: Whalen *et al.* (1987) Zr versus Ga/Al discriminant diagram of the Nhansipfe Granitic Orthogneiss plotting in the field of A- type granites (A).

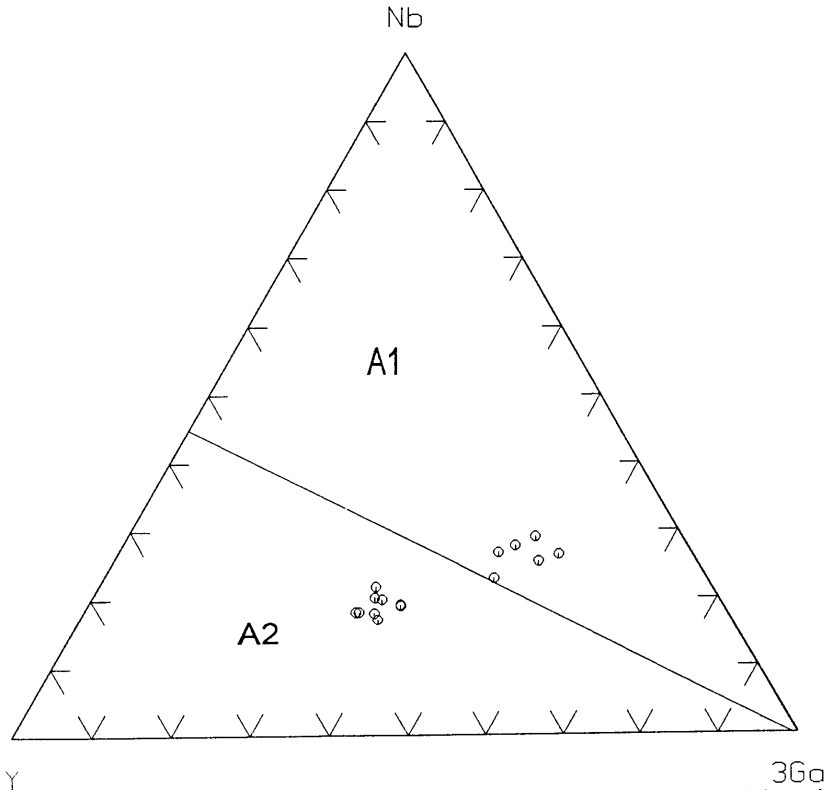

Figure 8.21: Discrimination of Nhansipfe Granitic Orthogneiss into A1 and A2 types granitoids (after Eby, 1992).

The discrimination of A-type granitoids using chemical criteria has been discussed by Eby (1990) who supported the criteria used by Whalen *et al.* (1987). He adds, however, that this discrimination is only reliable at SiO_2<65 wt% because at higher contents total alkali and CaO concentrations overlap. These parameters are largely met in this study. Eby (1992) further subdivided A-type granites into two groups, namely, A1, derived from sources chemically similar to those of oceanic island basalts, and A2 from sources similar to island arc or continental margin basalts (Eby, 1990, 1992). One way of assessing the existence of these two types of granites is the use of the incompatible elements Ga-Nb-Y discriminant diagram (Eby, 1992) which is shown in Figure 8.21 and in which the subdivision in A1 and A2 is evident. It must be emphasized that this triangular discriminant diagram can be used because the samples plot in the field of within-plate granite of Pearce *et al.* (1984) (Fig. 8.16) and in the A-type granitoids field in the Ga/Al diagram of Whalen *et al.*(1987) (Fig. 20) as required by Eby (1992).

A-type granitoids commonly have been perceived as being anorogenic, i.e., formed from magmatic processes unrelated to any orogen (eg. Pearce *et al.*, 1984). This concept has been critically challenged in recent times. For instance, Eby (1990) stated that A-type granitoids occur in within-plates or in plate margins during terminal stages of subduction-related orogeny. More recently, Windley (1993) discussed the problem related with anorogenic magmatism and suggests that a better understanding of this process can only be achieved if anorogenic magmatism is investigated in association with a local orogen.

The Nhansipfe Granitic Orthogneiss occurs within an area which includes the Proterozoic Chimoio Granodioritic Gneiss which plots in the volcanic-arc granites (VAG) field in the discriminant diagram of Pearce *et al.* (1984). It is, therefore, suggested that the Nhansipfe Granitic Orthogneiss has been formed from partial melting of a crust associated with/or produced during subduction related processes which are typical of a volcanic-arc tectonic environment.